




Article

Evaluation of the Impact of Drought and Saline Water Intrusion on Rice Yields in the Mekong Delta, Vietnam

Huynh Vuong Thu Minh ¹, Kim Lavane ², Tran Van Ty ³, Nigel K. Downes ¹, Tran Thi Kim Hong ⁴
and Pankaj Kumar ^{5,*}

¹ Department of Water Resources, CENRes, Can Tho University, Can Tho City 900000, Vietnam

² Department of Environmental Engineering, CENRes, Can Tho University, Can Tho City 900000, Vietnam

³ College of Engineering, Can Tho University, Can Tho City 900000, Vietnam

⁴ Department of Environment and Natural Resources, CENRes, Can Tho University, Can Tho City 900000, Vietnam

⁵ Institute for Global Environmental Strategies, Hayama 240-0115, Kanagawa, Japan

* Correspondence: kumar@iges.or.jp; Tel.: +81-46-855-3858 (ext. 3058)

Abstract: The Mekong delta is Vietnam's premier rice growing region, forming the livelihood basis for millions of farmers. At the same time, the region is facing various challenges, ranging from extreme weather events, saline water intrusion, and other anthropogenic pressures. This study examines how saline water intrusion and drought have affected rice yield in the Vietnamese Mekong Delta (VMD). Applying the Standardized Precipitation Index (SPI) and the maximum and minimum values of annual average salinity, we spatially examine the effects of drought and saline water intrusion on rice yields over a 40-year period (1980–2019). Our results highlight that 42% of the natural land area of the VMD has experienced increased drought occurrence during the winter-spring (WS) rice cropping season, while certain inland regions have additionally experienced increased drought occurrence during the summer-autumn (SA) rice cropping season. The Tri Ton Station, which has a significant Sen's slope of -0.025 and a p -value of 0.05 , represents an upstream semi-mountainous part of the delta, indicative of a rising severity of reoccurring drought. It should be noted that the yield decreases during the summer-autumn season as the positive SPI_{SA} increases. Salinity, on the other hand, is associated with SPI_{WS} during the winter-spring season. Our results highlight the need for improved evidence-based planning and investments in priority adaptation for both sustainable water infrastructure and to improve system resilience.

Keywords: drought; saline water intrusion; Standardized Precipitation Index; rice yield; Mekong Delta; adaptation



Citation: Minh, H.V.T.; Lavane, K.; Ty, T.V.; Downes, N.K.; Hong, T.T.K.; Kumar, P. Evaluation of the Impact of Drought and Saline Water Intrusion on Rice Yields in the Mekong Delta, Vietnam. *Water* **2022**, *14*, 3499. <https://doi.org/10.3390/w14213499>

Academic Editor: Manuel Esteban Sastre De Vicente

Received: 16 September 2022

Accepted: 28 October 2022

Published: 1 November 2022

Publisher's Note: MDPI stays neutral with regard to jurisdictional claims in published maps and institutional affiliations.



Copyright: © 2022 by the authors. Licensee MDPI, Basel, Switzerland. This article is an open access article distributed under the terms and conditions of the Creative Commons Attribution (CC BY) license (<https://creativecommons.org/licenses/by/4.0/>).

1. Introduction

Drought is a recurring climatic feature [1,2] that poses a serious threat to society [3]. It is frequently regarded as the most complex, yet least understood, of all climatic hazards [4–6]. Droughts differ from other natural hazards, such as floods, tropical cyclones, and earthquakes, as they are typically slow onset hazards [2,7–9]. Drought is defined as a shortfall in precipitation relative to what is considered to be expected normally over a season or a longer period of time, as well as the inability to sustain natural environmental flows and meet societal needs due to water scarcity and declining quality [2,5]. Moreover, despite improvements in forecasting, drought is still considered unpredictable [10]. Precipitation deficit is the most important driving factor for drought; however, it is still challenging to exactly pinpoint when a drought begins and ends [2,5]. As such, drought is usually related to a long and sustained period in which water availability becomes scarce [11], and as such, is also referred to as a creeping phenomenon [1,9]. In the context of climate change, a better understanding of drought mechanisms, improved monitoring and early warning systems are urgently needed to deal with both devastating and cascading

effects in the future [8]. At a regional scale, drought indices are commonly used to monitor hydrological conditions [12]. Several alternative indicators and indices have been proposed to quantify meteorological drought, but the Standardized Precipitation Index (SPI), created by McKee et al. (1993, 1995) [13,14], is one of the most often used [15]. The SPI was chosen by the World Meteorological Organization [16] as a drought indicator in 2009, and it was subsequently recommended to researchers and policymakers for estimating the effects and repercussions of meteorological drought on agricultural output and livelihoods to different geographical regions [17–23], including Vietnam [24–26].

The agricultural sector is the world's largest water user, accounting for roughly 70% of total global freshwater consumption. This is expected to increase to 90% by 2050, far beyond the predicted level of water availability [27,28]. Water demand for agricultural production in the Vietnamese Mekong Delta (VMD), one of the largest rice producing regions in the world, is sourced from rainfall, as well as 60% from the Mekong River. Here, agricultural water demand in 2100 is expected to be two to three times greater than that of 2000 [29]. Moreover, due to the low and flat terrain, its geography, and tropical monsoon climate, the VMD is extremely vulnerable to the impacts of climate change and saline water intrusion, which results in soil degradation and freshwater scarcity. The extent of affected land is expected to increase over the coming decades [30].

The current literature provides only a small number of studies addressing the spatio-temporal assessment of drought and saline water intrusion. Yin et al. (2021) [31] mapped global-scale maize drought risk in the context of climate change and undertook a drought risk assessment of China's mid-season paddy rice. Besides this, other studies have investigated drought adaptation and coping strategies, for example, in the Turkana Pastoralists of Northern Kenya [32]; in the USA [33]; and coastal Bangladesh [34]. This is in addition to studies of saline intrusion into the aquifers of the North American coastal region [35], or lessons learnt in water management from California [36].

The Mekong Delta in Vietnam is the world's third largest delta, home to nearly 18 million people, whose main source of income is agriculture and aquaculture production. Moreover, the substantial contamination of surface water prevents much of its use for domestic and agricultural tasks [37–39]. The freshwater resources are also strongly influenced by hydroelectric dam development in the upstream Mekong River system, which often causes a serious shortage of flow during the dry season to the downstream areas [40–42]. Moreover, the VMD recently suffered the most severe droughts and saline intrusion in the past 100 years, in both the 2015–2016 and 2019–2020 seasons. It should be noted that drought and saltwater intrusion not only affects the availability of fresh water for domestic use, but also disrupts production and cause crop losses. Here, water acts as a crucial driver for the vulnerability of local people in terms of water availability and future interactions between both the anthropogenic and hydrological systems. As a result, a comprehensive and effective hydro-meteorological management plan for the Mekong Delta region is required. Despite its great importance, very little robust scientific information is available to address the issues of climate change, saline intrusion, and drought and their impacts on rice yield in the VMD using an integrated approach [43,44]. With the aforementioned knowledge gap, this study applies an integrated approach to address the complex interactions of hydro-meteorological hazards, salt water intrusion and agricultural productivity. This approach is highly novel as it addresses the complex nexus interaction between food-water-climate change. This study has adopted equations and tools commonly used, which are not data intensive, yet provide robust scientific outcomes. Since the majority of countries in the Global South suffer from issues of data scarcity, this study highlights how to utilize the minimum available data for meaningful scientific works and policy relevant information for the sustainable and resilient development of an agricultural area located in a deltaic plain.

2. Methods

2.1. Study Area

The VMD is located in the monsoon region of Southeast Asia, with two distinct seasons; the rainy season roughly coincides with the summer, lasting from April to November. The activity and irregularity of the sea air masses, together with the activity of the monsoon and the equatorial-tropical disturbances therein, dominate and determine the weather changes in this region, whose consequences often result in extraordinary natural disasters, including drought [45].

The locations of 14 meteorological stations and four salinity stations are shown in Figure 1. Total daily rainfall was collected for the years 1978 to 2019, and daily salinity maximum and minimum data were collected from 2000 to 2019. The monthly salinity was collected from three stations along the eastern coast (Vam Kenh Station is located at the Mekong River estuary, Ben Trai Station is located along Co Chien River—a branch of Mekong's estuary, and Tran De Station located at Bassac River estuary). Salinity data were collected from one station on the western coast (Xeo Ro Station, located along the Cai Lon River about 8 kilometers from the river's mouth) and four stations on the eastern coast (Vam Kenh, Ben Trai, Tran De, and Xeo Ro). Between 2000 and 2019, the mean salinity maximum was 15.6 g/L, 16 g/L, 12.7 g/L, and 11.8 g/L, whereas the mean salinity minimum at those locations was 11.9 g/L, 5.1 g/L, 5.8 g/L, and 7.2 g/L, respectively.

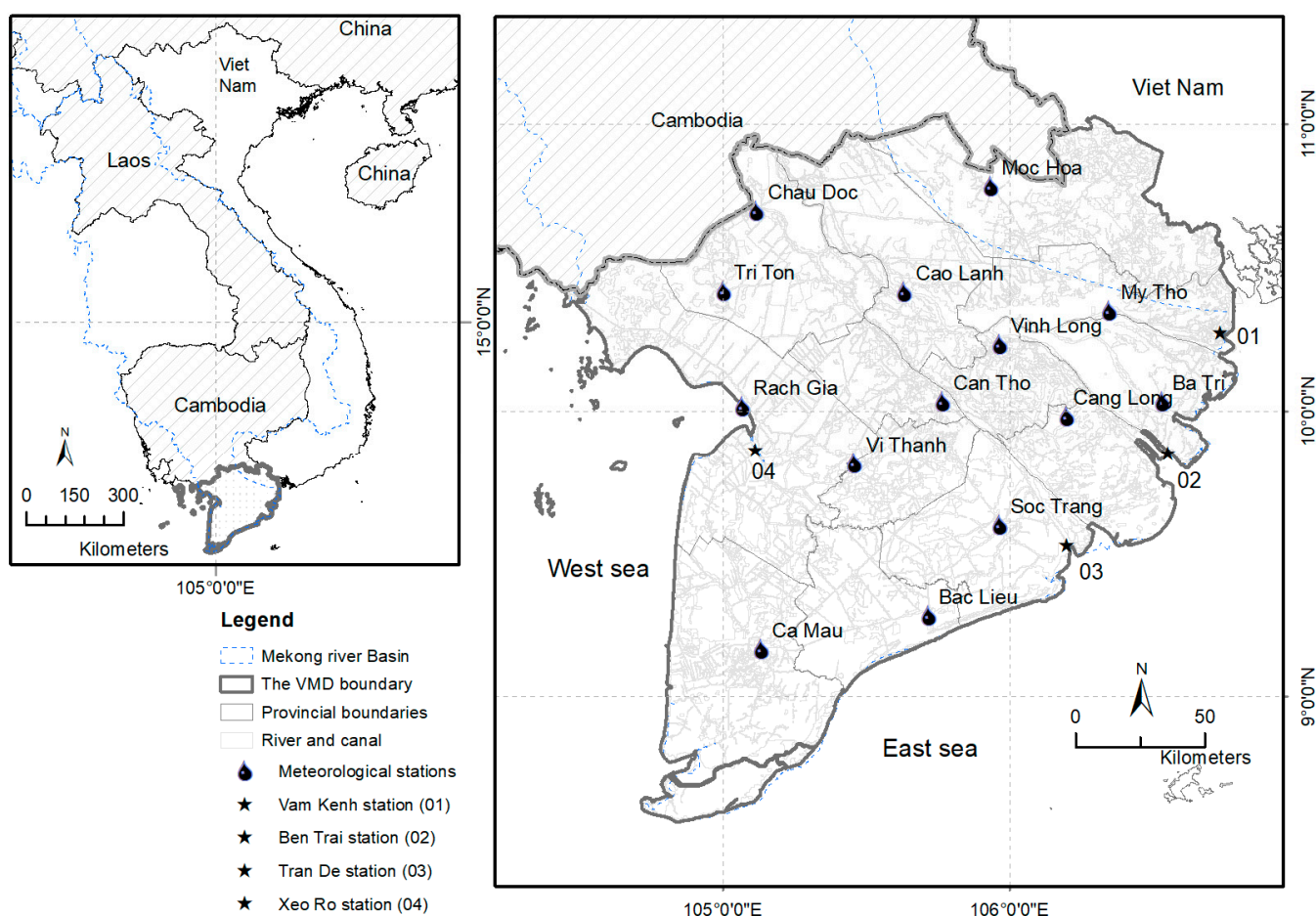


Figure 1. The location of the 14 meteorological stations and salinity stations (Vam Kenh, Ben Trai, Tran De, and Xeo Ro) utilized in the Vietnamese Mekong Delta.

In comparison to the normal distribution, SPI displays rainfall deficit. A meteorological drought condition is determined using the SPI at a 1-month temporal scale and is defined as the shortage of rain over a period of around 1 month. It is suggested to use the SPI

indicator on a scale of 3 to 9 months for agro-arid situations. The SPI may also depict hydrological arid conditions on a longer time range, from 12 to 48 months. Therefore, monthly precipitation values were used to calculate the SPI at multiple timescales. The drought criteria used in this study area were as follows:

- (i) Drought levels were calculated for 1-month and 12-month periods, and seasonal rice cropping (summer–autumn and winter–spring) over the 40-year dataset;
- (ii) Trend of droughts, and the maximum number of sequential arid years using trends in the SPI 12-month from the Mann–Kendall test and Sen’s slope [46];
- (iii) Cluster analysis and Thiessen were conducted for spatial analysis using SPI 12-month and SPI 1-month;
- (iv) Drought characteristics, such as drought frequency, length, and severity, were examined, as well as probability analysis;
- (v) The Pearson correlation technique were conducted the relationship between SPI seasons indices with saline water intrusion and rice yields.

2.2. SPI Calculation and Classification

Monthly rainfall data were collected from the aforementioned 14 stations for the 40-year period 1980–2019. The SPI values were calculated using McKee et al. (1993), for various time scales: 1-monthly, 12-month, time series seasons (summer–autumn and winter–spring). A positive or negative SPI value indicates an excess or deficit compared with the mean precipitation, respectively. Originally, McKee et al. (1993, 1995) [13,14] proposed drought begins when $SPI = 0$, although two later assessments by Agnew (2000) and Łabedzki (2007) [47,48] suggest that drought conditions start at $SPI = -1$. In this study, we used the SPI-based drought classification for Vietnam, in which $SPI = -0.25$ signifies the onset of drought conditions [24]. Drought indicators were classified into 10 hazard classes of moisture and drought: very slight, slight, moderate, severe, and extreme drought. SPI was calculated for each period with the SPI thresholds, as shown in Equation (1), and SPI values for different drought conditions, as shown in Table 1.

$$SPI_i = \frac{(R_i - \bar{R}_i)}{\sigma_i} \quad (1)$$

where, R_i is the total precipitation within the period, \bar{R}_i is the average precipitation in the period and, σ_i is the standard deviation.

Table 1. Vietnam’s SPI-based classification of the drought includes the category and value.

Drought Level	SPI Values	Drought Level	SPI Values
Normal	0–0.24	Normal	(−0.24)–0
Very slightly wet condition	−0.49	Very slight drought	(−0.49)–(−0.25)
Slightly wet condition	0.5–0.99	Slight drought	(−0.99)–(−0.5)
Moderately wet condition	1–1.44	Moderate drought	(−1.44)–(−1)
Severely wet condition	1.5–1.99	Severe drought	(−1.99)–(−1.5)
Extremely wet condition	>2	Extreme drought	<(−2)

2.3. SPI Trend Estimation Using the Mann–Kendall Test and Sen’s Slope Estimation

The application of the seasonal Mann–Kendall test was used for the piezometric time series data to enable further data interpretation for drought conditions. The magnitude of the slope was computed using the Sen’s slope test, as shown in Equation (2) [49].

$$S_k = \sum_{i=1}^n S_i \quad (2)$$

Kendall’s S statistic S_i for each season is summed to form the overall statistic, S_k . Mann–Kendall statistics provide an indication of whether a trend exists and, if so, whether

the trend is positive or negative based on range between -1 and 1 for each pair of data points, depending on the sign of the difference between the values. The Mann–Kendall equation, which is based on the value of S statistic, calculated using the equations shown as Equation (3).

$$S = \sum_{i=1}^{n-1} \sum_{j=i+1}^n \text{sgn}(x_j - x_i) \quad (3)$$

where x_i and x_j are sequential data values, n is the length of time series, and:

$$\text{sgn}(x_j - x_i) = \begin{cases} 1 & \text{if } (x_j - x_i) > 0 \\ 0 & \text{if } (x_j - x_i) = 0 \\ -1 & \text{if } (x_j - x_i) < 0 \end{cases} \quad (4)$$

Mann (1945) and Kendall (1975) [46,50] stated that when $n \geq 8$, S is almost normally distributed with the following mean and variance:

$$E(S_k) = 0 \quad (5)$$

The value of S near zero, positive and negative implies no significant, upward, and downward trends, respectively. The magnitude of S measures the strength of the trend. Note that if the absolute value of S is greater than the critical value of S indicates that trends are statistically significant.

$$\text{Var}(S_k) = \frac{1}{18} \left[\frac{n(n-1)(2n+5)}{\sum_{i=1}^n t_i(t_i-1)(2t_i+5)} \right] \quad (6)$$

where t_i is the number of ties of the extent i , and n is the number of observations in the set. The standard Z_{sk} statistic is calculated as follows:

$$Z_{sk} = \begin{cases} \frac{S_k-1}{\sqrt{\text{Var}(S_k)}} S_k > 0 \\ 0 & S_k = 0 \\ \frac{S_k+1}{\sqrt{\text{Var}(S_k)}} S_k < 0 \end{cases} \quad (7)$$

where Z_{sk} pursues the standard normal distribution with $\mu = 0$ and $\delta = 1$. The Sen's slope was used to determine magnitude of the trend. Z statistic is formed and compared with a critical point from the standard normal distribution. Besides this, the magnitude of a time series trend was evaluated by a simple non-parametric procedure developed by Sen, T_i is between any two values of a time series, which gives a total of $n(n-1)/2$ pairs of data could be calculated by:

$$T_i = \frac{x_j - x_i}{j - i} \quad (8)$$

where x_j and x_i are values at time j and i ($1 < i < j < n$), n is the number of data. The median of these n values of T_i is represented as Sen's estimator of slope. The positive and negative values of T_i indicate the upward and downward trends in the time series, respectively.

2.4. SPI Spatial Pattern Analysis

For evaluating the spatial pattern of SPI 12-month and hence the drought, first Agglomerative Hierarchical Clustering (AHC) was applied to the data from the 14 meteorological stations during 1980–2019 using the time series data of SPI 12-month. The mean SPI 12-month and SPI 1-month drought values were displayed using Thiessen analysis, which has been applied in many previous studies [51–53]. The influenced zone of each station was specified by the Thiessen method [54,55]. Data analysis was performed through statistical software using an add-on for Excel (XLSTAT) version 2021 [56]. Spatial analysis between

the 14 meteorological stations was carried out using the time series of SPI values, which were classified by the AHC method using the following steps. Firstly, each point of data developed its own cluster on its own, as shown by the equation ($G_i = \{x_i\}$, ($i = 1, 2, \dots, n$)). Development of the distance matrix $D = (D_{ij})_{cc}$, where c denotes the number of clusters; second, estimate the distances between each pair of objects in each cluster. Third, combine the clusters that are closest to one another (by setting $c = c - 1$, assume they are G_p and G_q into a new cluster G_r with their elements as $G_p \cup G_q$). Fourth, consider the cluster number. If the class number c exceeds the desired number of clusters, return back to Step 2. Finally, as output, extract the clustering results [57].

The area weighted rainfall method with the Thiessen polygon method was used for spatial interpolation. This is based on the assumption that the values of unsampled locations are equal to the value of the nearest sampled point. This method is commonly used in the analysis of climatic data; when data are unavailable, the nearest meteorological stations are used [58–61]. The principle of the Thiessen polygon is quite simple [62]. Let P be a finite set of points in the Euclidean plane; Thiessen polygons are derived from a topological relationship between a set of points (x, y) in two-dimensional space (Mu, 2009) [62]. Mathematically, assume P is a finite set of points in the Euclidean plane, $P = \{p_1, \dots, p_n\}$, where $2 \leq n \leq \infty$. If x is any location in the planar space, then the Euclidean distance between x and p_i is $d_e(x, p_i)$. Let $T(p_i)$ denote the Thiessen polygon of the point p_i , then:

$$T(p_i) = \{x | d_e(x, p_i) \leq d_e(x, p_j) \text{ for all } j, j \neq i \text{ and } i, j \leq n\} \quad (9)$$

3. Results and Discussion

3.1. SPI 12-Month Spatiotemporal Drought Analysis for the VMD

The SPI 12-month drought was determined for the 14 meteorological stations over the 40-year period, in order to divide them into 5 clusters based on the SPI 12-month drought characteristics (Figure 2). As a result, for each cluster, a time series of SPI 12-month drought value trends from 1980 to 2019 is also shown (Figure 3).

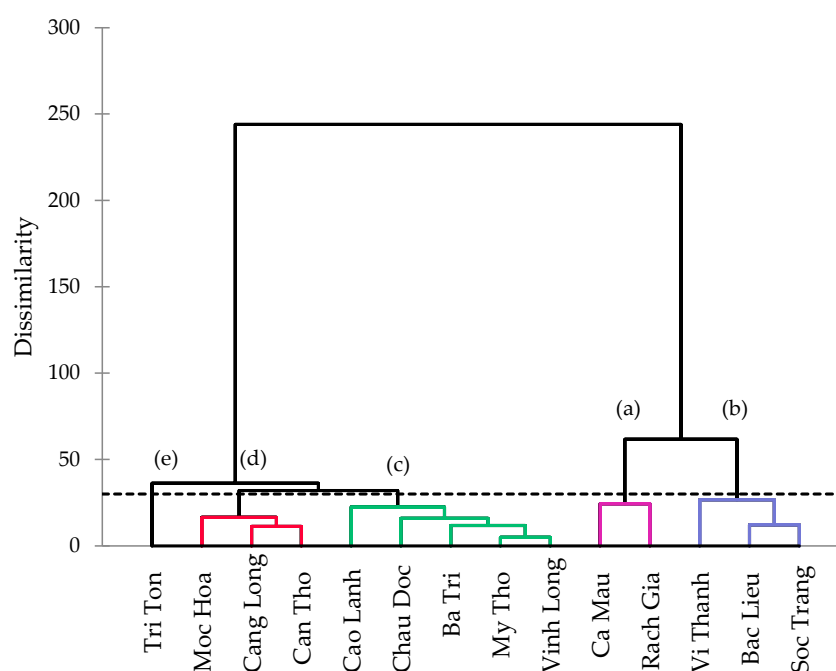


Figure 2. The 14 meteorological stations in the VMD were divided into five clusters based on the SPI 12-month drought over a period of 40 years: (a) Cluster No.1 (Ca Mau, Rach Gia), (b) Cluster No.2 (Vi Thanh, Bac Lieu, Soc Trang), (c) Cluster No.1 (Cao Lanh, Chau Doc, Ba Tri, My Tho, Vinh Long), (d) Cluster No.4 (Moc Hoa, Cang Long), and (e) Cluster No.3 (Tri Ton).

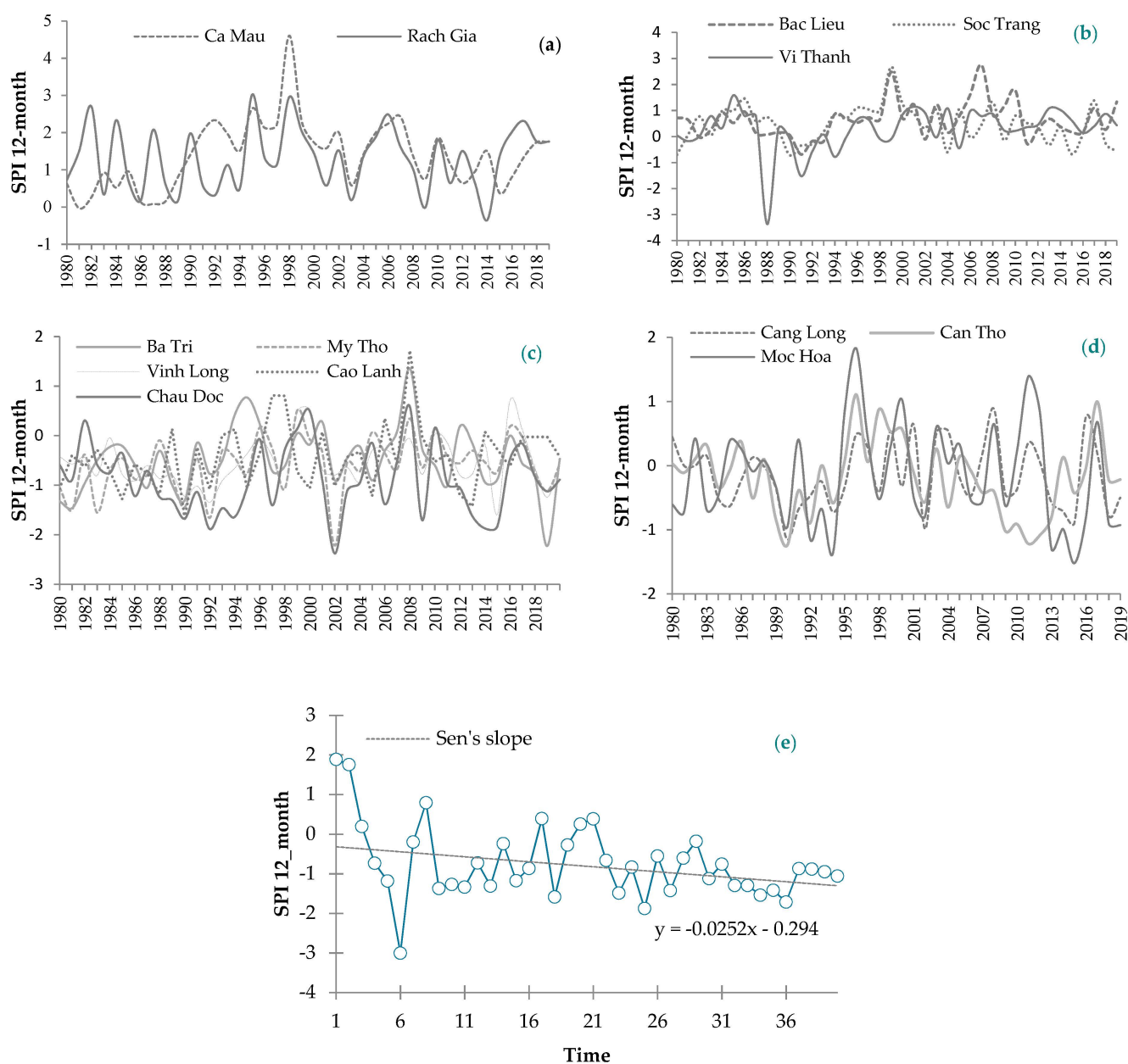


Figure 3. The SPI 12-month drought time series at 5 clusters, 1980–2019: (a) Cluster No.1, (b) Cluster No.2, (c) Cluster No.3, (d) Cluster No.4, (e) Cluster No.5 (only Tri Ton Station in cluster No.5 tends to increase the drought level at a p -value of 0.05 using Mann–Kendall test).

Figure 2 shows the AHC analysis results, which group the 14 meteorological stations into five clusters, in which two clusters consist of meteorological stations located in the coastal zones (clusters No.1 and 2), two clusters consist of meteorological stations located in the VMD's interior regions (clusters No.3 and 4), and one meteorological station represents a single station located in semi-mountainous terrain (cluster No.5).

Based on the SPI 12-month mean values of drought over a 40-year period, clusters No.1 and 2 were discovered to have positive SPI 12-month values (greater than 0). Cluster No.1 was categorized as moderately wet since its mean SPI 12-month drought value was high (1.35). When compared with the other cluster stations, Ca Mau and Kien Giang in cluster No.1 have higher mean SPI 12-month values, such as 1.4 and 1.3. Similar to cluster No.1, cluster No.2 was categorized as slightly wet, with a mean SPI 12-month drought value of 0.4. At each station in cluster No.2, the mean SPI 12-month drought values were determined

to be 0.28, 0.64, and 0.47 for Vi Thanh, Bac Lieu, and Soc, respectively. Because these two stations are near the coast, the SPI 12-month values of Bac Lieu and Soc Trang were slightly higher than those of Vi Thanh. Moreover, Figure 3b also highlights the extreme drought in Vi Thanh in 1988. Clusters No. 3, 4 and 5 have SPI 12 mean values that were negative (less than 0), which indicates that they have a tendency to be dry. The mean SPI 12-month drought value across Cluster No.3 stations was -0.37 , with individual values at the Cao Lanh, Chau Doc, Ba Tri, My Tho, and Vinh Long stations of -0.47 , -0.86 , -0.47 , -0.58 , and -0.54 , respectively. It was also noticed that the Chau Doc Station in Cluster No. 3 displayed the highest average level of drought compared to the others (Figure 3c). Besides that, Chau Doc and My Tho experienced an extreme drought in the year 2002. Although the characteristics of cluster No.4 was comprised stations with a negative mean SPI 12-month drought value, they were classified as normal condition (with mean SPI 12-month drought values of -0.17). It should be noted that cluster No.5 includes only a single station with an annual SPI 12-month drought value of -0.75 . At the stations in Tri Ton in cluster 5 and Chau Doc in cluster No.3, the SPI 12-month drought average values were comparable. The SPI 12-month value at the Tri Ton Station, in contrast to the Chau Doc Station, highlights a decreasing trend over time and with significantly higher variation for 40-year period 1980–2019.

Tri Ton Station in Cluster No.5 shows an increasing level of drought, with a significant Sen's slope of -0.025 and a p -value of 0.05 (Figure 3e). Moreover, despite the fact that the SPI 12-month drought detected increasing dryness at Moc Hoa, Can Tho, Cang Long, Chau Doc, and Soc Trang stations for the past 40 years, these trends were not statistically significant. Similar, the stations of Ca Mau, Rach Gia, Bac Lieu, Vi Thanh, Ba Tri, My Tho, Vinh Long, and Cao Lanh, the SPI 12-month drought tended to be more humid, but these trends were also not statistically significant.

Moreover, the results for the three meteorological stations, Cang Long, Can Tho, and Moc Hoa, all exhibited normal characteristics according to the drought catalogue of Vietnam. These findings have a high correlation with the AHC analysis results. Amongst different meteorological stations in the VMD, Rach Gia and Ca Mau showed the highest mean levels of rainfall in comparison to other regions. This is not surprising, given their coastal locations. This is in line with the AHC classification of cluster No.1 for Rach Gia and Ca Mau with wet conditions. The features of cluster No.2 (Bac Lieu, Soc Trang, and Vi Thanh) range from very slightly wet to moderately wet conditions. Although clusters No.3 and 5 both are part of the VMD's two clusters of droughts, cluster No.5 only contains Tri Ton Station, which has a unique drought characteristic relative to other stations. Cluster No.5's mean annual SPI tends to decline over time, indicating a tendency of intensifying drought conditions. In contrast to cluster No.5, the mean annual SPI of cluster No.3 varied from year to year (wet years alternating with dry years).

The Thiessen polygon interpolation method was used to spatially represent the mean SPI 12-month drought values (Figure 4).

As can be seen in Figure 4, interior areas tend to experience very slight to slight drought, while the coastal areas tend to display moderate to extremely wet conditions. To have a more in-depth understanding of the level of drought in the study area, it was required to take into account the monthly and seasonal distribution of rainfall deficiency. The Mann–Kendall test of 14 meteorological stations over a 40-year period using SPI 1-month is shown in Figure 5.

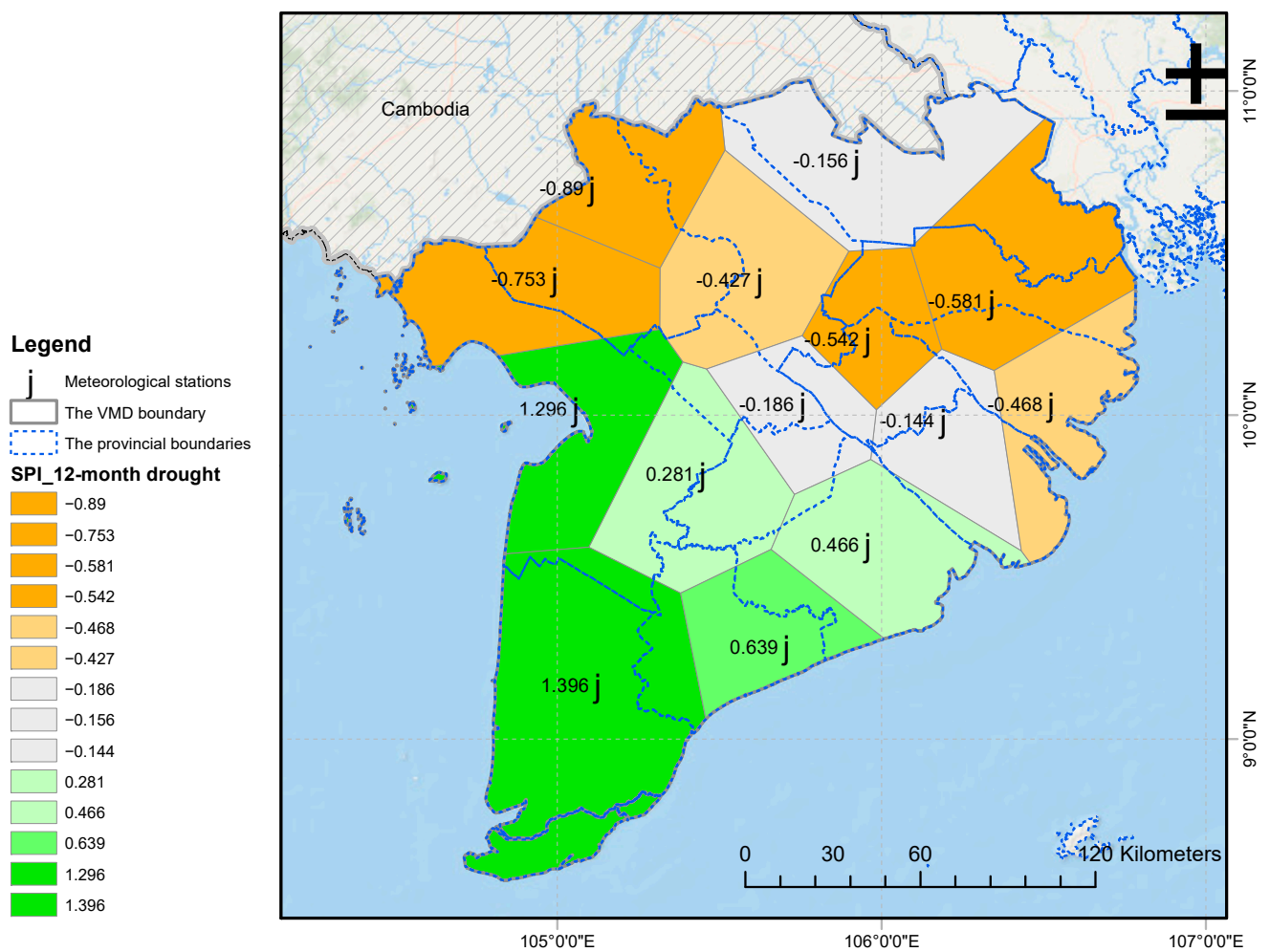


Figure 4. The mean SPI 12-month drought values using Thiessen polygon, during 1980 and 2019.

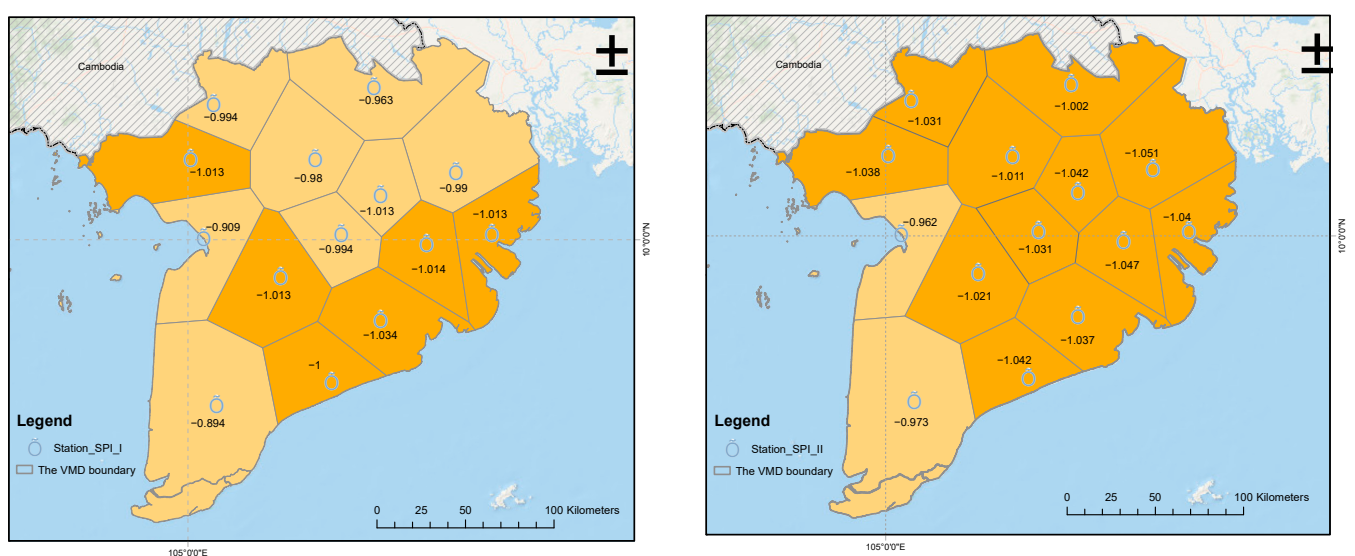


Figure 5. Cont.

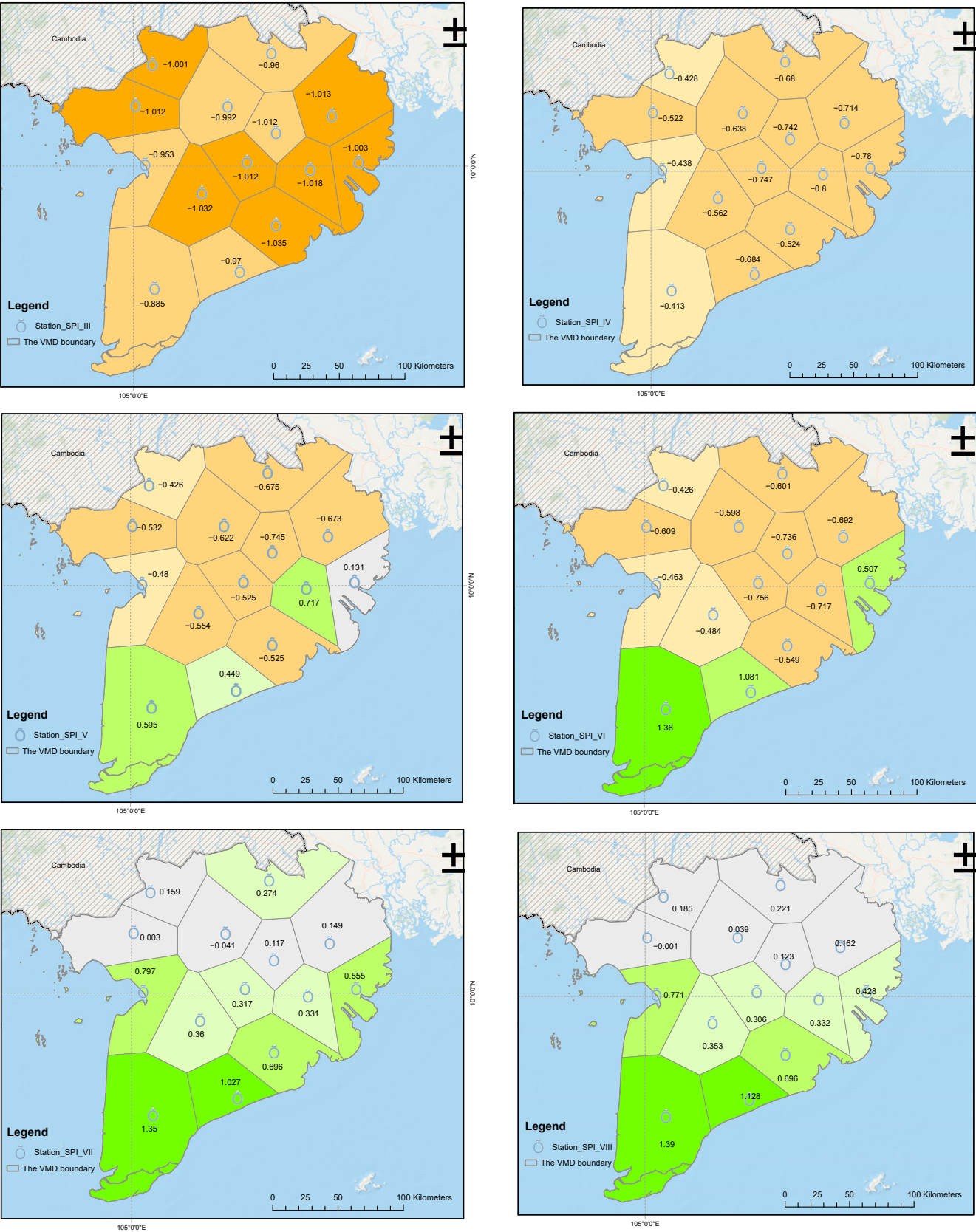


Figure 5. Cont.

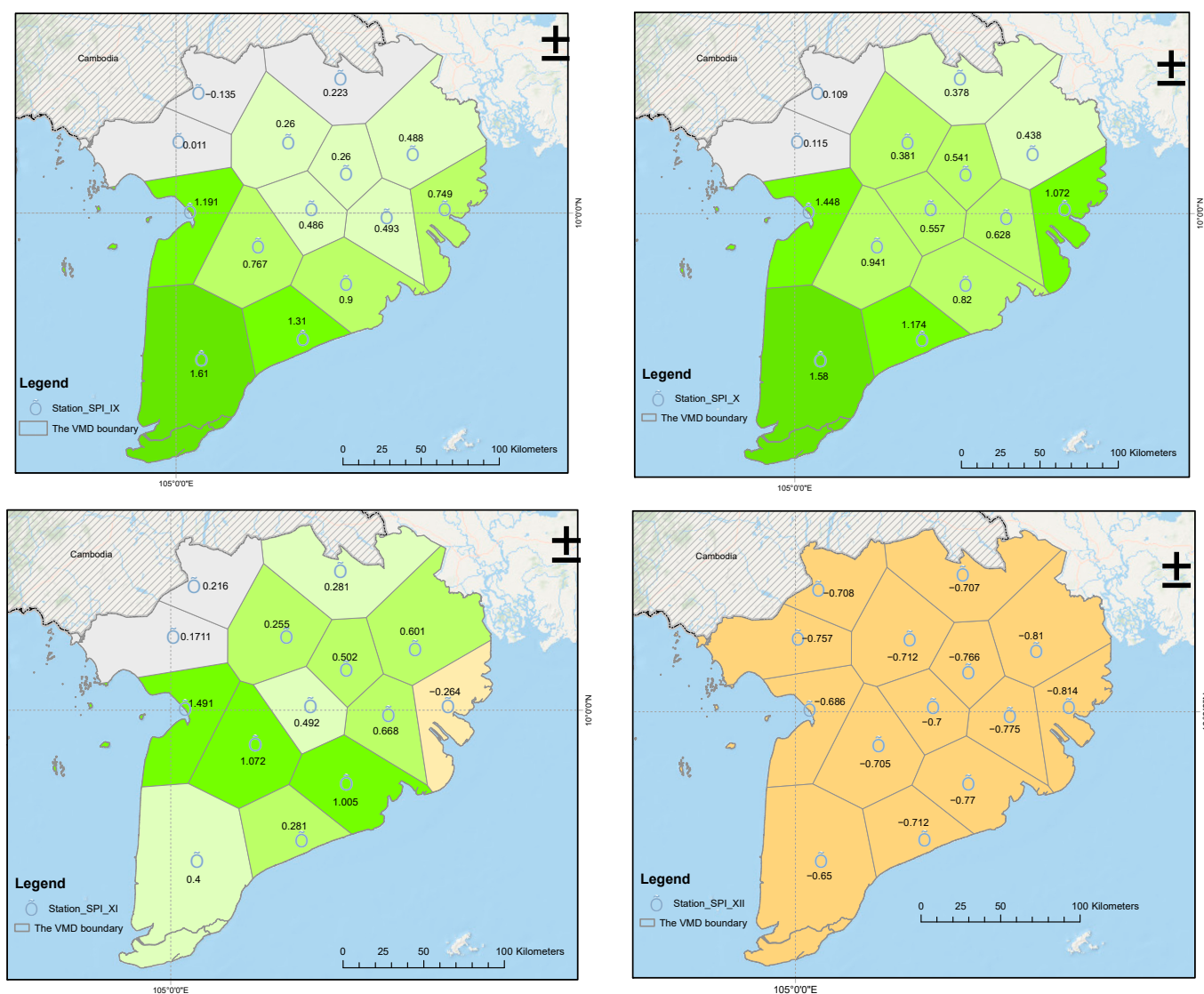


Figure 5. The mean SPI 1-month drought for the VMD using Thiessen polygon interpolation, during 1980 and 2019.

3.2. SPI 1-Month Spatiotemporal Drought Analysis for the VMD

The drought index enables drought monitoring at multiple timescales. The monthly distribution of rainfall was assessed, which is useful for agricultural water management. Figure 5 depicts the monthly distribution of rainfall deficit in the VMD.

Drought affects nearly the entire VMD every year from December to April in the dry season, with severity ranging from light to moderate. The VMD experienced the worst droughts on record, with moderate drought affecting 78% of the region and slight drought affecting 22% in the month of February. The light and moderate drought levels were observed for 62% and 34% of the total VMD area, respectively. A previous study also revealed that the VMD faced moderate drought in the years 2016 and 2020 [63,64]. Climate change and decreasing upstream flow volumes are determined to be the main factors affecting the VMD's drought conditions [64]. Although the wet season officially begins in May, the VMD typically experiences a very slight drought in both the months of May and June.

The area of the VMD affected by slight and very slight drought conditions in the month of May was 57% and 12%, respectively, and for June it was 60% and 19% for slight and very slight drought. The drought zone was seen in the semi-mountainous area of the

VMD as highlighted by Tri Ton meteorological station. Here, severe and slight drought conditions based on SPI 1-month values are shown in Figure 5. Similar to Tri Ton, Chau Doc Station showed similar results, despite the fact that the intensity of drought decreased compared to Tri Ton.

Nearly the entire VMD experienced humidity ranging from light to moderately wet (approximately 85%–89% of the land in the VMD) from July to October, with no signs of drought. For example, the calculated SPI 1-month values were 0.63, 0.68, 0.77, and 0.83 for July, August, September, and October, respectively. For the Ba Tri area (6% of the total natural land of the VMD region), the drought begins early in November, while the rest of the region experienced very slight wet conditions. Slight droughts are seen to occur over the entire VMD region from December onwards, and the cycle of drought is resumed.

3.3. Seasonal Drought Assessment in the VMD and Its Relationship with Rice Yield

Since wet years alternate with dry years in the VMD, the Mann–Kendall test found no evidence of increasing precipitation levels while only the Tri Ton Station displayed a decreasing trend of SPI 12-month during the 1980 and 2019 period with Kendall's tau values of -0.265 . Therefore, we expect to see a significant trend in the SPI season. The SPI seasonal trends show that for some meteorological stations, SPI values increased in the WS and decreased in the SA rice crop at a significance level of 0.05. In the SA rice cropping season, only Tri Ton Station exhibited a substantial decrease at the 0.05 level. However, a number of stations were found to have a significant increased precipitation trend and Figure 6 shows some stations with high Kendall's tau, such as station Ca Mau (0.301), Kien Giang (0.283), My Tho (0.349), Ba Tri (0.294) (Table A1).

In the WS rice cropping season, under a 5-year return period, the VMD would likely endure a slight drought ($SPI \leq -0.5$) over approximately 78% of its area. Whereas, a moderate drought ($SPI \leq -1$) affects approximately 86% of the VMD area once every 20–30 years. For wet conditions in the WS rice cropping season, for a 40-year return period, 57% of the VMD's land area, respectively, would experience moderate wet conditions ($SPI \geq 1$). Yet, only 4% of the VMD's land area is under a moderately wet condition, with a return period of 60 to 70 years.

It should also be noted that, the very slight drought and slight wet conditions tend to occur more frequently in the VMD during the WS rice cropping season. For example, about 52% and 39%, respectively, of the VMD's land area experiences very slight drought over a 3-year and a 4–5-year return period. In contrast, 73% and 19% of the VMD area are estimated to experience very slight wet conditions over a 4-year and a 9–10-year return period, respectively.

Approximately 43% and 33% of the land area are affected by slight drought and slight wet conditions once every 10–15 years. The moderate drought in the summer-autumn rice cropping season is a very rare occurrence. Only 16% and 66% of the VMD's land area are likely to experience a moderate drought with an average recurrence of a 30–50-year and a 100-year return period, respectively. In particular, Bac Lieu Station is likely to experience a repeated moderate drought situation at an average 1000-year return period, which would cover 5% of the region. In contrast, the moderate wet conditions would appear more often than moderate drought in the SA rice cropping season, with 37%, 24%, and 35% of the VMD area likely to face moderate wet conditions within a 40–50-year, 70–80-year, and 100-year return period, respectively.

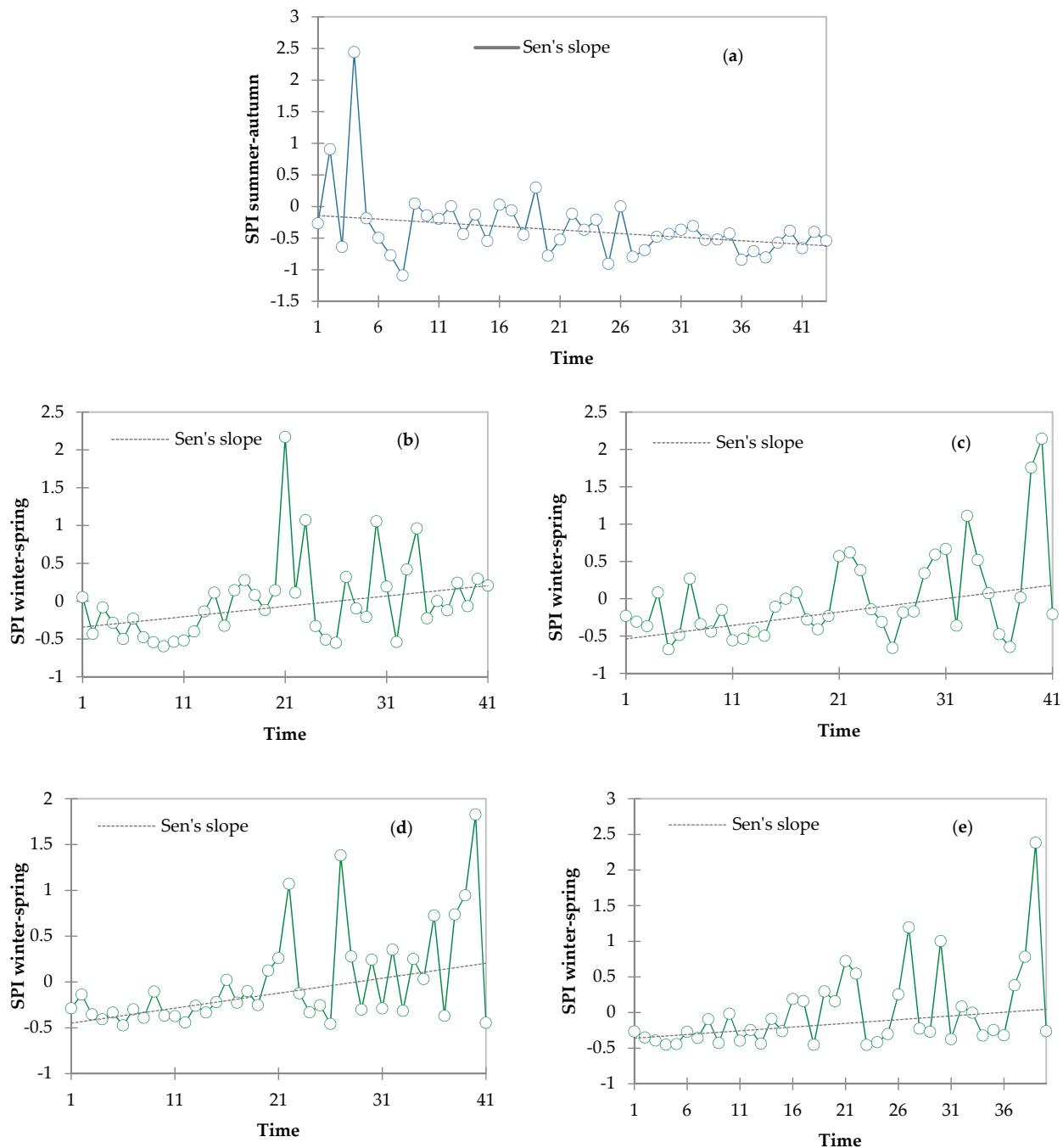


Figure 6. Trend analysis of seasonal drought events at selected meteorological stations over a 40-year period using the Mann–Kendall test and Sen's slope: (a) Tri Ton Station, (b) Ca Mau Station, (c) Kien Giang Station, (d) My Tho Station, and (e) Ba Tri Station. The results of the probability analysis and return periods are shown in Figure A1 (Ca Mau and Bac Lieu stations only) and Table 2. The return period is defined by $(T = 1/P)$ or $(T = 1/(1 - P))$ depending on P values, in which, P denotes the probability of occurrence or exceedance of an event and T denotes the return period. The value of the return period was used, based on how frequently droughts or wet periods occur. Table 2 shows a comprehensive summary for the occurrence of drought conditions for different cropping seasons and for different return periods. It was found that the VMD experiences very light droughts ($SPI \leq -0.25$) or very slight wet periods ($SPI \geq 0.25$) more frequently during the winter and spring months. Overall, on average, 97% of the entire study area will experience a very slight drought in a 3-year return period, and 96% of the area will experience a very slight wet period ($SPI \geq 0.25$) for the winter-spring rice cropping over a 4-year return period.

Table 2. Return period (N, year) at various drought levels for SA and WS rice cropping seasons.

The Summer-Autumn Rice Cropping Season						
Name of Station	Return Period (Year) SPI ≤ -1	Return Period (Year) SPI ≤ -0.5	Return Period (Year) SPI ≤ -0.25	Return Period (Year) SPI ≥ 0.25	Return Period (Year) SPI ≥ 0.5	Return Period (Year) SPI ≥ 1
Bac Lieu	1000	12	4	4	9	54
Ba Tri	104	6	4	3	5	110
Ca Mau	118	8	3	4	8	44
Cang Long	123	11	4	4	11	120
Can Tho	122	20	5	1	20	121
Cao Lanh	34	7	3	4	8	38
Chau Doc	78	7	3	4	8	78
Moc Hoa	121	8	3	4	8	60
My Tho	100	10	3	10	5	139
Rach Gia	123	11	3	4	9	64
Soc Trang	101	10	4	4	12	105
Vinh Long	109	14	5	4	11	106
Vi Thanh	75	10	4	4	10	65
Tri Ton	53	2	2	9	16	50
The Winter-Spring Rice Cropping Season						
Bac Lieu	43	7	3	5	11	73
Ba Tri	25	5	3	4	9	41
Ca Mau	26	6	3	4	9	39
Cang Long	28	6	3	4	9	37
Can Tho	33	7	3	4	9	44
Cao Lanh	22	5	3	4	7	28
Chau Doc	24	5	3	4	9	38
Moc Hoa	44	8	4	4	10	60
My Tho	34	6	3	3	5	33
Rach Gia	20	5	3	4	7	27
Soc Trang	30	6	3	4	8	40
Vinh Long	30	7	3	4	9	40
Vi Thanh	25	6	3	4	8	32
Tri Ton	24	5	3	4	8	33

The very slight drought, as well as very slight wet conditions, are seen to be a common occurrence in the VMD. However, very slight drought occurs more often, and the affected area in both seasons is also spatially larger than that in the very slight wet conditions. In general, the SA rice cropping season showed wet conditions more frequently than the WS rice cropping season, whereas the WS rice cropping season experienced drought conditions more frequently than the SA season. It should be noted that the higher positive SPI indicates more rain in the SA rice cropping season, which could affect rice yield. Therefore, the Pearson correlation was used to identify the relationship between SPI indices and saline water intrusion with rice yield, as is shown in Figure 7.

For the SA rice cropping season, we found that the correlation between the average rice yield and the average SPI_SA in the VMD was 0.65 at a significance level of $\alpha = 0.05$. Moreover, the salinity (Smin and Smax) at Vam Kanh Station (Co Chien River) and the annual winter-spring rice yield in the VMD was also found to be correlated with a correlation value of 0.82 for Smax and 0.8 for Smin, respectively; at a significance level of $\alpha = 0.05$. It should be noted that during the summer-autumn season, the yield decreases as the positive SPI increases. Salinity, on the other hand, is associated with SPI_WS during the WS season. However, air temperature, hydraulic irrigation works, and rice farming practices have the potential to be confounding variables that can affect rice yield. It was reported that the rice production decreased by 70% during the 2016 drought, when compared with the previous year [64]. Previous research has also revealed livelihood vulnerability under the impact of drought in Asian countries [22,65]. Going forward, further research is needed to find innovative solutions to adapt as the extent and severity of the drought worsens.

The sustainability of water resources is dependent on interconnected physical, chemical, biological, and human processes, all of which have an impact on the quantity and quality of available water supplies [37]. To manage saltwater intrusion, one must first

understand the extent of the issue, as well as the physical mechanisms (or modes) by which saltwater intrusion occurs as a result of natural and human activities [36]. In order to effectively raise awareness of natural disasters and how to respond, and in order to make effective use of water resources, public outreach must be expanded. Furthermore, equipment must support drought and salinity monitoring and warning systems. To ensure long-term resource sustainability, the scientific and political communities must combine their mutual interests and forge a coordinated plan that the public understands and embraces.

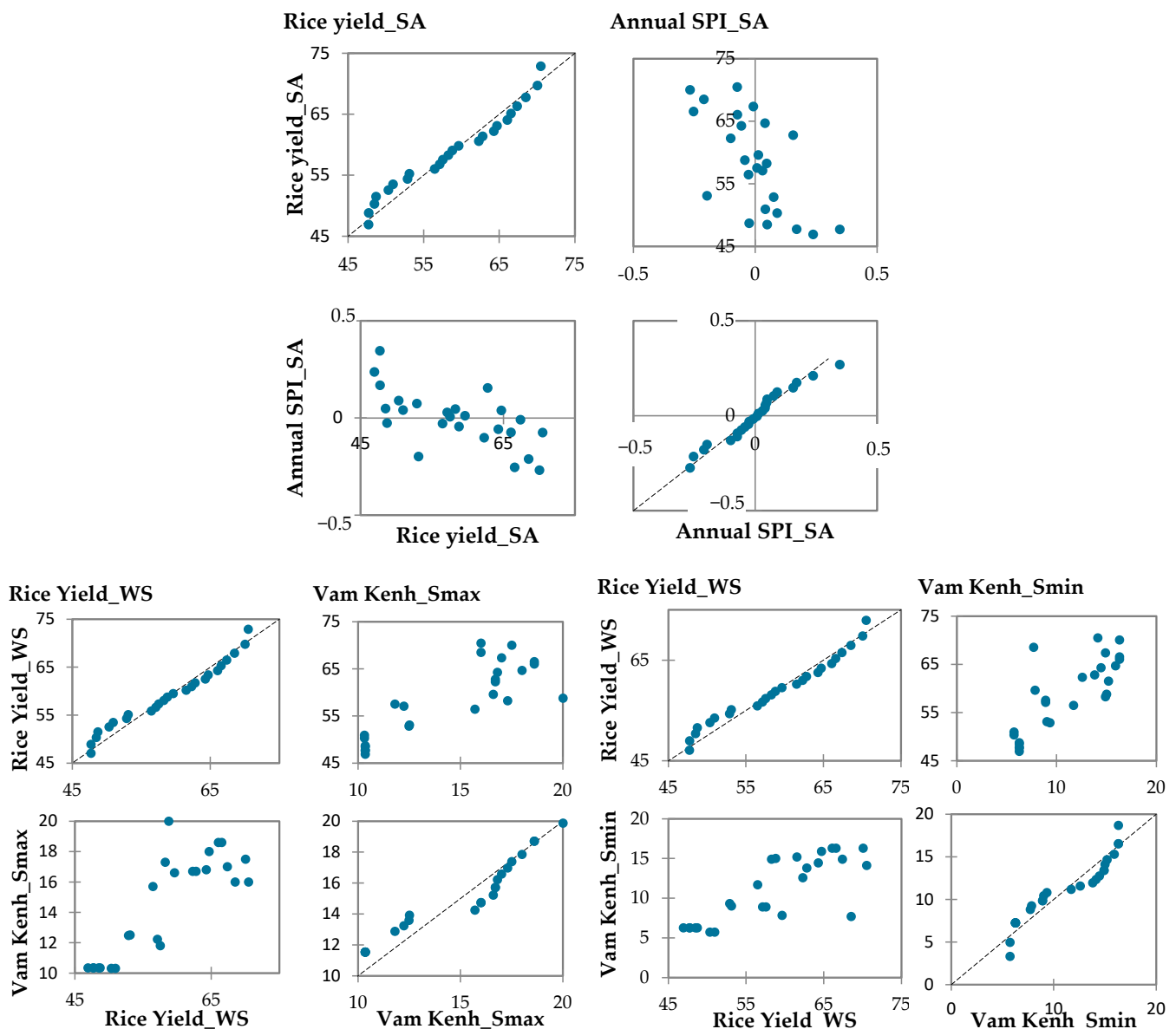


Figure 7. The Pearson correlation between mean rice yield in the summer-autumn rice cropping season and winter-spring rice cropping season with annual SPI season (SA and WS) and salinity at coastal stations (Vam Kenh, Tra Vinh, and Xeo Ro).

Considering the severity of the impacts of saltwater intrusion and hydro-meteorological hazards like drought, in terms of both socio-economic losses and human welfare, this study has used an integrated approach to address the complex interaction of both issues and agricultural productivity. This approach is highly novel, as it used transdisciplinary approach to address this complex nexus issue of interaction between food-water-climate change. This study adopted the equations and tools that are commonly used but are not data-intensive, yet provides robust scientific outcomes. Since most of the developing

countries in Asia or the Global South has a common issue of data scarcity, this study will provide a guideline about how to use minimal available data for meaningful scientific works and policy-relevant information for decision-makers.

4. Conclusions

Based on the SPI 1-month, SPI 12-month, and SPI seasonal drought patterns, it was seen that wet periods and drought vary by region (coastal, interior, and semi-mountainous areas). These were grouped into five clusters with comparable drought characteristics: two clusters in the interior region, two clusters in the coastal zone, and one cluster in the semi-mountainous region. According to the findings of the SPI season time series analysis for the VMD, drought tended to worsen between 1980 and 2019 in both the summer-autumn and winter-spring seasons. At a significance level of 0.05, there is a trend of increasing drought severity, particularly in the semi-mountainous region (represented by the Tri Ton meteorological Station). Similar to the interior and coastal regions of the VMD, the representative stations (Can Tho and Cang Long) frequently face dry conditions during the SA cropping season. It should be noted that 42% of the VMD's land area is susceptible to drought during the WS rice cropping season, which can be considered as a disadvantage, because at this time saline intrusion propagates deep into the VMD's rivers and canals, coupled with low discharge volumes, as well as low rainfall.

Furthermore, a relationship between rice yield and SPI was discovered for the SA rice cropping seasons. Our findings indicate that the yield of rice in the SA season will decline with increased rainfall. Furthermore, we discovered a strong relationship between the average rice yield in the VMD and the average yearly salinity (S_{min} and S_{max}) at the Vam Kenh Station during the WS rice cropping season. Overall, the risk of reduced rice yields in the WS rice cropping season is greater than it is for the SA rice cropping season due to the limited rainfall and increased saline intrusion. Considering the huge impacts of droughts and salt water intrusion on rice yields, it is also imperative to undertake an analysis of loss and damages from an economic viewpoint in future works. Moreover, as loss of rice yields results in substantial impacts to human health, both mentally, as well as physically, future works should incorporate a nexus analysis incorporating the all important health elements.

Author Contributions: Conceptualization, H.V.T.M., K.L., T.V.T. and P.K.; methodology, H.V.T.M., K.L., T.V.T., N.K.D., T.T.K.H. and P.K.; data curation, H.V.T.M., T.V.T. and P.K.; writing—original draft preparation, H.V.T.M., K.L., T.V.T., N.K.D., T.T.K.H. and P.K.; writing—review and editing, H.V.T.M., K.L., T.V.T., N.K.D. and P.K. All authors have read and agreed to the published version of the manuscript.

Funding: This research work is partly funded by the Vietnam Ministry of Education and Training (research code: B2021-TCT-13). This project is also supported from the Japan Science and Technology Agency, e-Asia JRP, under the project entitled 'Integration of traditional and modern bioproduction systems for a sustainable and resilient future under climate and ecosystem changes (ITMoB)'. This research was supported by Japan Science and Technology Agency (JST), as a part of the Abandonment and Rebound: Societal Views on the Landscape- and Land-Use Change and their Impacts on Water and Soils (ABRESO) project under Belmont Forum. This publication is supported by the Asia Pacific Network for Global Change Research (APN), under collaborative regional research programme (CRRP), with project reference number CRRP2019-01MY-Kumar.

Institutional Review Board Statement: Not applicable.

Informed Consent Statement: Not applicable.

Data Availability Statement: Not applicable.

Conflicts of Interest: The authors declare no conflict of interest.

Appendix A

Table A1. Mann-Kendall test trend for rice cropping SPI seasons.

Station	Summer-Autumn				Winter-Spring			
	Kendall's Tau	S	Var (S)	p-Value (Two-Tailed)	Kendall's Tau	S	Var (S)	p-Value (Two-Tailed)
Ca Mau	0.038	30	7366.667	0.735	0.301	235	7365.667	0.0064 **
Rach Gia	−0.029	−24	7926.667	0.796	0.283	232	7926.667	0.009 **
Soc Trang	−0.059	−51	8514.333	0.588	0.104	89	8509.667	0.340
Vi Thanh	0.134	115	8514.333	0.217	0.352	303	8512.333	0.001 **
Bac Lieu	0.077	63	7925.667	0.486	0.159	130	7926.667	0.147
Cao Lanh	0.108	84	7366.667	0.334	0.153	119	7365.667	0.169
Chau Doc	0.108	84	7366.667	0.334	−0.023	−21	9128.333	0.834
Ba Tri	−0.087	−75	8514.333	0.423	0.294	253	8514.333	0.006 **
My Tho	0.085	70	7926.667	0.438	0.349	286	7926.667	0.001 **
Vinh Long	0.215	168	7366.667	0.052	0.236	184	7366.667	0.03 *
Moc Hoa	−0.116	−100	8513.333	0.283	0.137	118	8513.333	0.205
Cang Long	−0.087	−75	8514.333	0.423	0.294	253	8514.333	0.0063 **
Can Tho	−0.052	−47	9130.333	0.630	0.238	215	9130.333	0.025 *
Tri Ton	−0.265	−239	9130.333	0.013 *	0.205	185	9130.333	0.054

Note: * Signification codes: $0.001 < "****" < 0.01 < "***" < 0.05$.

Appendix B

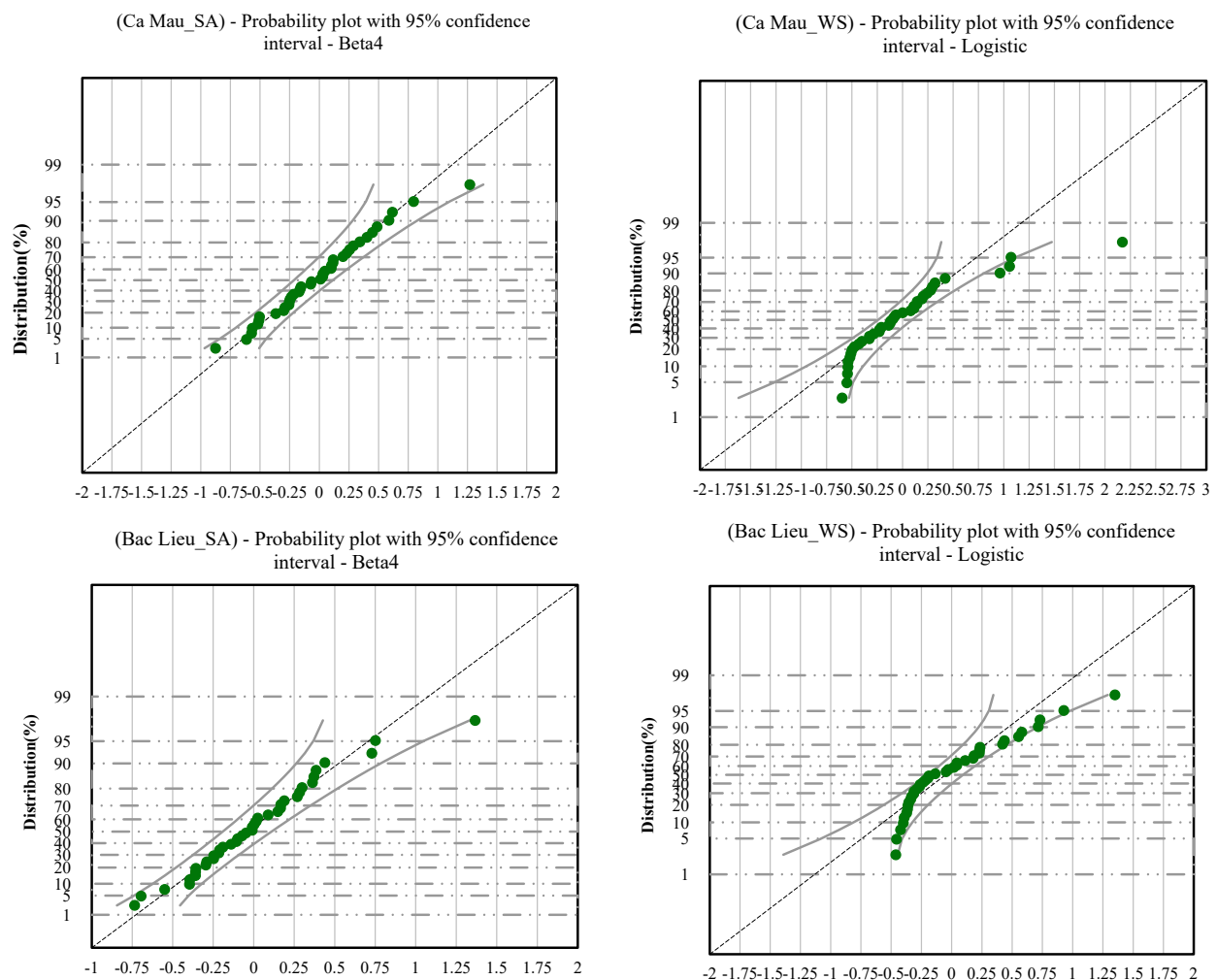


Figure A1. Probability plot for SPI seasons at Ca Mau and Bac Lieu stations.

References

1. Senbeta, T.B.; Romanowicz, R.J. Evaluating Historical Drought Using Different Drought Indices and Data Processing Schemes. In Proceedings of the 1st IAHR Young Professionals Congress, Online, 17 November 2020.
2. Sivakumar, M.V. *Agricultural Drought—WMO Perspectives*; World Meteorological Organization: Geneva, Switzerland, 2011; p. 24.
3. Wilhite, D.A.; Glantz, M.H. Understanding: The Drought Phenomenon: The Role of Definitions. *Water Int.* **1985**, *10*, 111–120. [\[CrossRef\]](#)
4. Hagman, G.; Beer, H.; Bendz, M.; Wijkman, A. *Prevention Better than Cure. Report on Human and Environmental Disasters in the Third World*; Swedish Red Cross: Stockholm, Sweden, 1984; p. 187.
5. Wilhite, D. Chapter 1 Drought as a Natural Hazard: Concepts and Definitions. In *Drought: A Global Assessment*; Drought Mitigation Center Faculty Publications: Lincoln, NE, USA, 2000; Volume 69, pp. 3–18. Available online: <https://digitalcommons.unl.edu/cgi/viewcontent.cgi?article=1068&context=droughtfacpub> (accessed on 6 April 2022).
6. Hahn, M.B.; Riederer, A.M.; Foster, S.O. The Livelihood Vulnerability Index: A Pragmatic Approach to Assessing Risks from Climate Variability and Change—A Case Study in Mozambique. *Glob. Environ. Chang.* **2009**, *19*, 74–88. [\[CrossRef\]](#)
7. Zarei, A.R.; Shabani, A.; Moghimi, M.M. Accuracy Assessment of the SPEI, RDI and SPI Drought Indices in Regions of Iran with Different Climate Conditions. *Pure Appl. Geophys.* **2021**, *178*, 1387–1403. [\[CrossRef\]](#)
8. Hayes, M.; Svoboda, M.; Wall, N.; Widhalm, M. The Lincoln Declaration on Drought Indices: Universal Meteorological Drought Index Recommended. *Bull. Am. Meteorol. Soc.* **2011**, *92*, 485–488. [\[CrossRef\]](#)
9. Tannehill, I.R. *Drought, Its Causes and Effects*; LWV: Philadelphia, PA, USA, 1947; Volume 64, ISBN 0038-075X.
10. Soleimani, H.; Ahmadi, H.; Zehtabian, G. Comparison of Temporal and Spatial Trend of SPI, DI and CZI as Important Drought Indices to Map Using IDW Method in Taleghan Watershed. *Ann. Biol. Res.* **2013**, *4*, 46–55.
11. Dracup, J.A.; Lee, K.S.; Paulson, E.G., Jr. On the Definition of Droughts. *Water Resour. Res.* **1980**, *16*, 297–302.
12. Jain, V.K.; Pandey, R.P.; Jain, M.K.; Byun, H.-R. Comparison of Drought Indices for Appraisal of Drought Characteristics in the Ken River Basin. *Weather Clim. Extrem.* **2015**, *8*, 1–11. [\[CrossRef\]](#)
13. Mishra, A.K.; Singh, V.P. A Review of Drought Concepts. *J. Hydrol.* **2010**, *391*, 202–216. [\[CrossRef\]](#)
14. McKee, T.B.; Doesken, N.J.; Kleist, J. The Relationship of Drought Frequency and Duration to Time Scales. In Proceedings of the 8th Conference on Applied Climatology, Anaheim, CA, USA, 17–22 January 1993; American Meteorological Society: Boston, MA, USA, 1993; Volume 17, pp. 179–183.
15. McKee, T.B. *Drought Monitoring with Multiple Time Scales*; American Meteorological Society: Boston, MA, USA, 1995.
16. Svoboda, M.; Fuchs, B.A. *Handbook of Drought Indicators and Indices*; Integrated Drought Management Tools and Guidelines Series; World Meteorological Organization: Geneva, Switzerland, 2016; Volume 2.
17. Lloyd-Hughes, B.; Saunders, M.A. A Drought Climatology for Europe. *Int. J. Climatol. J. R. Meteorol. Soc.* **2002**, *22*, 1571–1592. [\[CrossRef\]](#)
18. Li, L.; She, D.; Zheng, H.; Lin, P.; Yang, Z.-L. Elucidating Diverse Drought Characteristics from Two Meteorological Drought Indices (SPI and SPEI) in China. *J. Hydrometeorol.* **2020**, *21*, 1513–1530. [\[CrossRef\]](#)
19. Wang, L.; Chen, W. A CMIP5 Multimodel Projection of Future Temperature, Precipitation, and Climatological Drought in China. *Int. J. Climatol.* **2014**, *34*, 2059–2078. [\[CrossRef\]](#)
20. Osuch, M.; Romanowicz, R.J.; Lawrence, D.; Wong, W.K. Trends in Projections of Standardized Precipitation Indices in a Future Climate in Poland. *Hydrol. Earth Syst. Sci.* **2016**, *20*, 1947–1969. [\[CrossRef\]](#)
21. Masoudi, M.; Afrough, E. Analyzing Trends of Precipitation for Humid, Normal and Drought Classes Using Standardized Precipitation Index (SPI), a Case of Study: Fars Province, Iran. *Int. J. AgriSci.* **2011**, *1*, 85–96.
22. Lei, Y.; Wang, J.; Luo, L. Drought Risk Assessment of China's Mid-Season Paddy. *Int. J. Disaster Risk Sci.* **2011**, *2*, 32–40. [\[CrossRef\]](#)
23. Romero-Jiménez, E.; García-Valdecasas Ojeda, M.; Rosa-Cánovas, J.J.; Yeste, P.; Castro-Díez, Y.; Esteban-Parra, M.J.; Gámiz-Fortis, S.R. Hydrological Response to Meteorological Droughts in the Guadalquivir River Basin, Southern Iberian Peninsula. *Water* **2022**, *14*, 2849. [\[CrossRef\]](#)
24. Thắng, N.V.; Khiêm, M.V. Nghiên cứu đánh giá ảnh hưởng của điều kiện khô hạn theo chỉ số SPI cho khu vực Đồng bằng Sông Cửu Long. *Tạp chí Khí tượng Thủy văn* **2017**, *6*, 1–9.
25. Ty, T.V.; Hoai, D.T.T.H.; Minh, H.V.T. Mapping Meteorological Drought in the Mekong Delta under Climate Change. *Can Tho Univ. J. Sci.* **2015**, *2025*, 1980–2012.
26. Hồng, N.V.; nh Thơ, P.T.; Giai, N.S. Khả năng sử dụng chỉ số SPI trong đánh giá ảnh hưởng của điều kiện khô hạn và ẩm ướt đến năng suất lúa ở vùng Cần Thơ-Hậu Giang. *Tạp Chí Khoa học Biến đổi khí hậu* **2018**, *5*, 36–42.
27. FAO. *Guidelines on Irrigation Investment Projects*; Food and Agriculture Organization: Rome, Italy, 2018; p. 120.
28. Tondel, F.; D'Alessandro, C.; Dekeyser, K. *The Effects of Major Economies' Policies on Climate Action, Food Security and Water in Developing Countries*; ECDPM: Maastricht, The Netherlands, 2022.
29. Smyle, J.; Cooke, R. *Comprehensive Environment and Climate Change Assessment in Viet Nam*; International Fund for Agricultural Development IFAD: Rome, Italy, 2014.
30. Setia, R.; Gottschalk, P.; Smith, P.; Marschner, P.; Baldock, J.; Setia, D.; Smith, J. Soil Salinity Decreases Global Soil Organic Carbon Stocks. *Sci. Total Environ.* **2013**, *465*, 267–272. [\[CrossRef\]](#)
31. Yin, Y.; Gao, Y.; Lin, D.; Wang, L.; Ma, W.; Wang, J. Mapping the Global-Scale Maize Drought Risk Under Climate Change Based on the GEPIC-Vulnerability-Risk Model. *Int. J. Disaster Risk Sci.* **2021**, *12*, 428–442. [\[CrossRef\]](#)
32. Opiyo, F.; Wasonga, O.; Nyangito, M.; Schilling, J.; Munang, R. Drought Adaptation and Coping Strategies among the Turkana Pastoralists of Northern Kenya. *Int. J. Disaster Risk Sci.* **2015**, *6*, 295–309. [\[CrossRef\]](#)

33. Fu, X.; Tang, Z.; Wu, J.; McMillan, K. Drought Planning Research in the United States: An Overview and Outlook. *Int. J. Disaster Risk Sci.* **2013**, *4*, 51–58. [\[CrossRef\]](#)
34. Abedin, M.; Habiba, U.; Shaw, R. Community Perception and Adaptation to Safe Drinking Water Scarcity: Salinity, Arsenic, and Drought Risks in Coastal Bangladesh. *Int. J. Disaster Risk Sci.* **2014**, *5*, 110–124. [\[CrossRef\]](#)
35. Barlow, P.M.; Reichard, E.G. Saltwater Intrusion in Coastal Regions of North America. *Hydrogeol. J.* **2010**, *18*, 247–260. [\[CrossRef\]](#)
36. Kretsinger Grabert, V.; Narasimhan, T. California's Evolution toward Integrated Regional Water Management: A Long-Term View. *Hydrogeol. J.* **2006**, *14*, 407–423. [\[CrossRef\]](#)
37. Thu Minh, H.V.; Avtar, R.; Kumar, P.; Le, K.N.; Kurasaki, M.; Ty, T.V. Impact of Rice Intensification and Urbanization on Surface Water Quality in An Giang Using a Statistical Approach. *Water* **2020**, *12*, 1710. [\[CrossRef\]](#)
38. Giao, N.T. Surface Water Quality in Aquacultural Areas in An Giang Province, Vietnam. *Int. J. Environ. Agric. Biotechnol.* **2020**, *5*, 1054–1061. [\[CrossRef\]](#)
39. Chea, R.; Grenouillet, G.; Lek, S. Evidence of Water Quality Degradation in Lower Mekong Basin Revealed by Self-Organizing Map. *PLoS ONE* **2016**, *11*, e0145527. [\[CrossRef\]](#)
40. Le Huy, B.; Xuan, H.N.; Van, N.T.; Le, H.H. The Dangers of the Construction of Hydroelectric Dams Upstream of the Mekong River Adversely Effect on the Ecosystems and Livelihoods of People in the Mekong Delta, Viet Nam. *Environ. Chall.* **2021**, *5*, 100349. [\[CrossRef\]](#)
41. Tran, T.; Thang, N.; Huong, H.; Khiem, N.; Hien, N.; Ha Phong, D. *Climate Change and Sea Level Rise Scenarios for Viet Nam*; IPCC Summary for Policymakers: Geneva, Switzerland, 2016.
42. Dat, T.Q.; Kanchit, L.; Thares, S.; Trung, N.H. Modeling the Influence of River Discharge and Sea Level Rise on Salinity Intrusion in Mekong Delta. In Proceedings of the 1st Environment Asia International Conference, Thailand, Bangkok, 22–25 March 2011; Volume 35, pp. 685–701.
43. Loc, H.H.; Van Binh, D.; Park, E.; Shrestha, S.; Dung, T.D.; Son, V.H.; Truc, N.H.T.; Mai, N.P.; Seijger, C. Intensifying Saline Water Intrusion and Drought in the Mekong Delta: From Physical Evidence to Policy Outlooks. *Sci. Total Environ.* **2021**, *757*, 143919. [\[CrossRef\]](#)
44. Tran, D.D.; Dang, M.M.; Du Duong, B.; Sea, W.; Vo, T.T. Livelihood Vulnerability and Adaptability of Coastal Communities to Extreme Drought and Salinity Intrusion in the Vietnamese Mekong Delta. *Int. J. Disaster Risk Reduct.* **2021**, *57*, 102183. [\[CrossRef\]](#)
45. Tín, N.Đ. Xây Dựng Công Nghệ Dự Báo Hạn Khí Tượng ở Khu Vực Đồng Bằng Sông Cửu Long. *Tạp Chí Khoa Học Kỹ Thuật Thủ Lợi Và Môi Trường Số* **2012**, *37*, 2012.
46. Mann, H.B. Nonparametric Tests against Trend. *Econom. J. Econom. Soc.* **1945**, *13*, 245–259. [\[CrossRef\]](#)
47. Agnew, C. Using the SPI to Identify Drought. *Natl. Drought Mitig. Cent. Univ. Neb. Linc.* **2000**, *1*, 6–12.
48. Łabędzki, L. Estimation of Local Drought Frequency in Central Poland Using the Standardized Precipitation Index SPI. *Irrig. Drain. J. Int. Comm. Irrig. Drain.* **2007**, *56*, 67–77. [\[CrossRef\]](#)
49. Hirsch, R.M.; Slack, J.R.; Smith, R.A. Techniques of Trend Analysis for Monthly Water Quality Data. *Water Resour. Res.* **1982**, *18*, 107–121. [\[CrossRef\]](#)
50. Kendall, M. *Rank Correlation Methods*, 4th ed.; Charles Griffin: London, UK, 1975.
51. Hartomo, K.D.; Sri Yulianto, J.; Gumilangeng, E. Spatial Model of Koppen Climate Classification using Thiessen Polygon Optimization Algorithm. *J. Theor. Appl. Inf. Technol.* **2018**, *96*, 2.
52. William, K.H.; Hutomo, K.D. The Natural Disaster Prone Index Map Model in Indonesia Using the Thiessen Polygon Method. *INTENSIF J. Ilm. Penelit. Dan Penerapan Teknol. Sist. Inf.* **2021**, *5*, 148–160. [\[CrossRef\]](#)
53. Zhao, S.; Wang, K.; Liu, C.; Jackson, E. Investigating the Effects of Monthly Weather Variations on Connecticut Freeway Crashes from 2011 to 2015. *J. Saf. Res.* **2019**, *71*, 153–162.
54. Asrari, E.; Masoudi, M.; Hakimi, S.S. GIS Overlay Analysis for Hazard Assessment of Drought in Iran Using Standardized Precipitation Index (SPI). *J. Ecol. Environ.* **2012**, *35*, 323–329. [\[CrossRef\]](#)
55. Fiedler, F.R. Simple, Practical Method for Determining Station Weights Using Thiessen Polygons and Isohyetal Maps. *J. Hydrol. Eng.* **2003**, *8*, 219–221. [\[CrossRef\]](#)
56. Boots, B.N. Weighting Thiessen Polygons. *Econ. Geogr.* **1980**, *56*, 248–259. [\[CrossRef\]](#)
57. Zhou, S.; Xu, Z.; Liu, F. Method for Determining the Optimal Number of Clusters Based on Agglomerative Hierarchical Clustering. *IEEE Trans. Neural Netw. Learn. Syst.* **2016**, *28*, 3007–3017. [\[CrossRef\]](#) [\[PubMed\]](#)
58. Tatalovich, Z.; Wilson, J.P.; Cockburn, M. A Comparison of Thiessen Polygon, Kriging, and Spline Models of Potential UV Exposure. *Cartogr. Geogr. Inf. Sci.* **2006**, *33*, 217–231. [\[CrossRef\]](#)
59. Ian, H. *An Introduction to Geographical Information Systems*; Pearson Education: Nodia, India, 2010; ISBN 81-317-3193-6.
60. Richter, A.; Ng, K.T.; Karimi, N.; Wu, P.; Kashani, A.H. Optimization of Waste Management Regions Using Recursive Thiessen Polygons. *J. Clean. Prod.* **2019**, *234*, 85–96. [\[CrossRef\]](#)
61. Mu, L. Thiessen Polygon. In *International Encyclopedia of Human Geography*; Kitchin, R., Thrift, N., Eds.; Elsevier: Amsterdam, The Netherlands, 2009; pp. 231–236, ISBN 978-0-08-044910-4.
62. Park, E.; Loc, H.H.; Van Binh, D.; Kantoush, S. The Worst 2020 Saline Water Intrusion Disaster of the Past Century in the Mekong Delta: Impacts, Causes, and Management Implications. *Ambio* **2022**, *51*, 691–699. [\[CrossRef\]](#)
63. Phan, V.H.; Dinh, V.T.; Su, Z. Trends in Long-Term Drought Changes in the Mekong River Delta of Vietnam. *Remote Sens.* **2020**, *12*, 2974. [\[CrossRef\]](#)

-
64. Sebastian, L.; Sander, B.; Simelton, E.; Zheng, S.; Hoanh, C.; Tran, N.; Buu, C.; Quyen, C.; Ninh, N. *The Drought and Salinity Intrusion in the Mekong River Delta of Vietnam-Assessment Report*; CGIAR Research Program on Climate Change, Agriculture and Food Security: Bogor, Indonesia, 2016. Available online: <https://ccafs.cgiar.org/resources/publications/drought-and-salinity-intrusion-mekong-river-delta-vietnam-assessment> (accessed on 6 April 2022).
 65. Thao, N.T.T.; Khoi, D.N.; Xuan, T.T.; Tychon, B. Assessment of Livelihood Vulnerability to Drought: A Case Study in Dak Nong Province, Vietnam. *Int. J. Disaster Risk Sci.* **2019**, *10*, 604–615. [[CrossRef](#)]